

Rehabilitation of Fire-damaged Reinforced-concrete Slabs Using Ferro-cement

Raneen Aldarf¹⁾, Muneeb Al-Allaf¹⁾, Abdulrazak Salem²⁾ and Hani Meree^{3)*}

¹⁾ School of Civil Engineering, Al-Baath University, Syria.

²⁾ School of Civil Engineering, Hama University, Syria.

³⁾ State Key Laboratory of Geohazard Prevention and Geoenvironment Protection, Chengdu University of Technology, Chengdu 610059, China.

* Corresponding Author. E-Mail: hani.meree@hotmail.com

ABSTRACT

This study was conducted to investigate the effect of strengthening with ferro-cement on the flexural behavior of two-way RC slabs after exposure to direct fire. Twelve reinforced-concrete slabs were exposed to direct fire for one hour and cooled with air and water. They were then rehabilitated with a layer of ferro-cement using different bonding patterns (surface roughening, SBR material and screws). The effect of these variables was studied on the load-deflection relationship, ultimate load capacity, stiffness, energy absorption, ductility factor and strains of the compressed zone. The results showed a significant improvement in all the investigated parameters, demonstrating the efficiency of ferro-cement strengthening in improving the behavior of the slabs. It contributed to increasing the ultimate load capacity and initial stiffness of the slabs and to preventing and arresting crack propagation after cracking and even after reaching collapse. The effectiveness of SBR material in ensuring the bonding between the surface of the damaged slabs and the reinforcement layer was also revealed.

KEYWORDS: Solid slab, Direct fire flame, Ferro-cement, Rehabilitation, SBR (styrene-butadiene rubber), Roughing.

INTRODUCTION

Reinforced concrete is a fundamental material in construction, but it can be damaged by fire. This can lead to a decrease in the load-bearing capacity of the structure and in some cases, even to partial or complete destruction. When concrete structures are exposed to fires, the materials within them burn, leading to the destruction of the internal fabric of the concrete and a change in its mechanical properties and the properties of the internal reinforcing steel. This results in a decrease in their strength and load-bearing capacity (Sulakhe and Awcha, 2019; Handoo and Agarwal, 2002; Mathew and Sureshbabu, 2021; Kanagaraj et al., 2023). As a result, it is necessary to assess the extent of damage in these structures and not demolish them. Instead, engineers resort to reinforcing, repairing and rehabilitating them.

One of the major challenges that structural engineers may face is developing a technique for rehabilitating concrete slabs to regain a portion of their integrity after prolonged exposure to fire. This is because the high costs associated with reinforcement materials, such as carbon fibers, glass fibers and steel meshes, as well as the difficulty of their application on the damaged and fragmented concrete surface due to fire, make them unsuitable for this purpose (Esmaelili et al., 2018; Obaidat, 2017). As a result, researchers have sought an alternative material that meets the desired conditions. These conditions include ease of use, cost-effectiveness (low cost), local availability, applicability to irregularly damaged surfaces and providing a high bond strength between the old damaged concrete surface and the new concrete surface. Ferro-cement is a type of reinforced concrete that is made up of multiple layers of wire mesh that are covered with a ferro-cement mortar. It is a versatile material that can be used to repair and rehabilitate concrete slabs that have been damaged by

Received on 4/8/2023.

Accepted for Publication on 1/12/2023.

fire. ferro-cement has several advantages over other reinforcement materials, such as carbon fibers, glass fibers and steel meshes. It is easier to use, more cost-effective and more readily available. It can also be applied to irregularly damaged surfaces and it provides a high bond strength between the old concrete surface and the new concrete surface. As a result, ferro-cement is a promising material for the rehabilitation of concrete slabs that have been damaged by fire. It is a cost-effective, versatile and easy-to-use material that can help restore the structural integrity of these slabs. In 1997, the committee of the American Institute (ACI) issued its guidance report, considering ferro-cement as a non-traditional technique that differs from reinforced concrete (Maharashtra, 2018; Saleem and Ashraf, 2008; Mourad, 2006; Lugowski, 2013; Shah, 1974; ACI, 2009; Salgia and Panganti, 2018).

Numerous research studies have contributed to highlighting the importance of ferro-cement in the reinforcement and rehabilitation of various structural elements, such as columns, beams and slabs. These studies have also aimed to investigate the mechanical properties of the constituent materials involved in its formation. Atwan (2015) conducted a performance evaluation of the mechanical properties of a ferro-cement-mortar specimen strengthening with multiple layers of wire mesh from one to six layers. The researcher found that reinforcing the specimen with 5 layers of wire mesh resulted in a 61.5% increase in compressive strength and a 205.21% increase in fracture toughness compared to the reference samples. Furthermore, it was possible to reduce the cement content in the specimen by approximately 20% when it was reinforced with a single layer of wire mesh. Furthermore, Long et al. (2011) mentioned that ferro-cement has evolved in its use since the beginning of the last century, particularly in strengthening and repairing damaged parts of structural elements. Ferro-cement is known as a thin cementitious layer reinforced with closely spaced layers of a relatively small-diameter wire mesh. This configuration provides enhanced resistance to compression, tension and fracture properties, making it suitable for practical applications in cementitious mortar. Peter (2008) found that the cementitious mortar of ferro-cement consists of a mixture of sand, binding material and water. The mechanical properties of the mortar depend on the nature of the binding material. The

cementitious mortar has been used as a bonding material in building units for walls and in surface protection for structural elements. Researchers investigated the effect of reinforcement and repair with ferro-cement on the behavior of reinforced-concrete columns, slabs and beams. They studied the impact of the thickness of the ferro-cement layer, the number of layers of the steel mesh and the compressive strength of the ferro-cement mortar on the maximum load-carrying capacity of the tiles, deflection-load relationships and crack patterns. The results demonstrated the effectiveness of ferro-cement repair and reinforcement in enhancing the performance of these slabs (Mabrouk et al., 2022; Fahmy et al., 2014; Shaaban et al., 2018; Sayhood et al., 2018). Mahmoud (2013) conducted laboratory experiments on a series of flat slabs strengthened with ferro-cement strips. The study examined the effect of the thickness of the cover layer, the type of wire mesh, the number of mesh layers and the strengthening method on the behavior of these slabs in resisting punching shear. The researcher found that the use of ferro-cement strips significantly helped increase the collapse load and stiffness of the slabs. It was also observed that ferro-cement can be used as an alternative repair technique to strengthen flat slabs against punching shear. Ahmed (2017) conducted laboratory experiments on several pre-damaged slabs, loaded up to 80% of the collapse load, as well as undamaged slabs. All the slabs were reinforced with a layer of ferro-cement, either reinforced with traditional steel reinforcement, wire mesh or carbon and glass fiber mesh. The researcher found that both repair methods and strengthening methods using a layer of ferro-cement showed effectiveness in enhancing the performance of the slabs. However, reinforcing with carbon fiber mesh yielded the best results among the different reinforcement methods. The bubbled concrete slabs exposed to high temperatures of 300 C° and 400 C° for half an hour and one hour and loaded until failure, were rehabilitated with carbon fibers (CFRP) by the researchers Waryosh and Hashim (2020). It was found that the rehabilitated bubbled slabs regained their original strength and the ultimate load capacity increased by a percentage of 79% to 105% compared to the control slabs. Haddad et al. (2011) conducted an investigation on the effect of rehabilitation using carbon fiber (CFRP), glass fiber (GFRP) and steel fiber-reinforced concrete (SFRC) on the behavior of heat-

damaged reinforced-concrete slabs. The researchers found that all rehabilitation methods were effective in restoring the slabs' original strength and increasing their stiffness.

The significance of this research is that it investigates the use of ferro-cement to rehabilitate fire-exposed slabs without the use of carbon fibers or other reinforcement materials. This is important, because it could provide a more cost-effective and sustainable way to repair fire-damaged structures. The problem that this research addresses is the need for more effective and affordable methods for rehabilitating fire-damaged slabs. Traditional methods of rehabilitation, such as the use of carbon fibers, can be expensive and time-consuming. Ferro-cement is a less affordable and sustainable alternative that could potentially provide the same level of performance. The results of this research could have a significant impact on the way how fire-damaged slabs are rehabilitated. If ferro-cement is shown to be an effective and reliable method of rehabilitation, it could become a more widely used alternative to traditional methods. This could save money and resources and could also help reduce the environmental impact of fire damage.

TEST PROGRAM

Model Design

The experimental work was conducted at the

Reinforced-concrete Laboratory in Syria. Twelve simply supported reinforced-concrete slabs were tested. The slabs had identical dimensions (1200×800×100) mm and similar material properties. The slabs were reinforced in both the long and short directions. A concentrated external force was applied at the center of each slab. Figure 1(a) illustrates the dimensions of the slabs and provides details about the reinforcement. The concrete slabs were categorized into three groups: reference, fire exposure and rehabilitation groups. The reference-group slabs were loaded until failure. The fire-exposure group slabs were loaded to 62% of the reference collapse load and then exposed to direct fire for one hour. Five of the fire exposure-group slabs were cooled by water spraying, while the other five were allowed to cool naturally in the air. Two of the fire-exposure group slabs were selected as burnt and cooled reference slabs. The rehabilitation-group slabs were fire-damaged slabs that were rehabilitated using ferro-cement with a thickness of 25mm. Different bonding patterns were used for the rehabilitation, including the adhesive material (SBR) and surface roughening for the damaged surface, eight bolts, twelve bolts and sixteen bolts. Table 1 provides a summarized overview of the tested samples, including their specifications and characteristics. Figure 1 (b) illustrates the bonding patterns utilized during the ferro-cement rehabilitation process of the damaged slabs.

Table 1. Tested slabs

Group	Specimen	Type of cooling	Bonding pattern
Group1	R-S	Control	-
Group2	RG1	Gradually(G)	-
	FG1		SBR and roughing surface
	FG2		SBR, roughing and 8bolts
	FG3		SBR and 12bolts
	FG4		SBR and 16bolts
Group3	RS1	Suddenly(S)	-
	FS1		SBR and roughing surface
	FS2		SBR, roughing and 8bolts
	FS3		SBR and 12bolts
	FS4		SBR and 16bolts

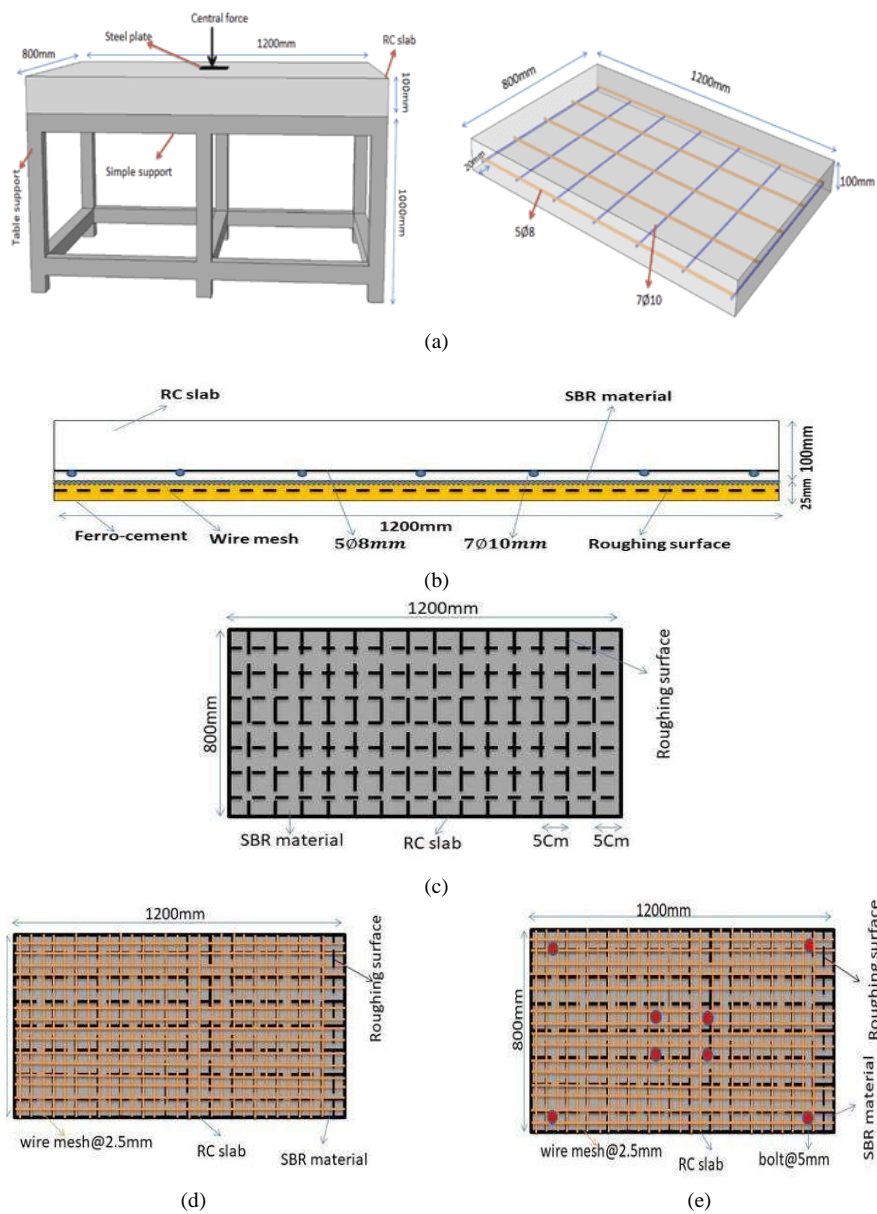


Figure 1): (a) Details of reference slabs, (b) Repairing slabs, (c) Roughing surface, bounding patterns of ferro-cement, (d) SBR and roughing surface, (e) SBR, 8 bolts and roughing surface, (f) SBR and 12 bolts and (g) SBR and 16 bolts

Mix Design and Material Properties

The concrete-mix proportions for the reinforced-concrete slabs and cylindrical specimens were carefully selected to ensure the quality and integrity of the specimens. The mix proportions were as follows: Cement: 1, Sand: 1.77, Coarse aggregate: 1.5, Gravel aggregate: 2, Crushed sand: 3 and water:0.54. The maximum nominal size of the aggregate used was 20mm. Clean white sand, passing through a no. 4.72 mm sieve with a sand equivalent of 74, was utilized.

Ordinary Portland cement with a density of 400 kg/m^3 was employed in the mixture. All the necessary laboratory tests were conducted, including sieve analysis of the aggregates, sand equivalent test for the sand, specific-gravity test and others, to ensure their compliance with the required specifications according to the American Society for Testing and Materials (ASTM) standards. The quality of the construction materials was ensured before the wooden molds were prepared and cleaned for casting the reinforced-concrete slabs. The

steel reinforcement bars were accurately cut to form the specific reinforcement mesh required for these slabs, with a cover-layer thickness of 20 mm. During the pouring process, a mechanical vibrator was used to eliminate any potential voids and ensure uniformity. Following the casting, the slabs were carefully moistened with water and then covered with burlap bags for a curing period of seven days. This curing process helps the concrete hydrate properly and enhances its strength and durability. After the curing period, the wooden molds were removed, revealing the finished slabs. Three cylindrical concrete samples were fabricated and cured for 28 days. The compressive strength of the concrete was determined to be 25MPa. Three samples of reinforcing steel were also tested, with yield stresses of 540MPa and 660MPa for 10mm- and 8mm- diameter steel, respectively.

Burning Process

The furnace is a metallic box with dimensions of (1000 x 800 x 1400) mm. It is insulated with glass wool and has two movable and two fixed walls. Two tubes with multiple heat sources are placed inside the furnace. The furnace is open from the top and bottom to ensure adequate ventilation. Concrete slabs were subjected to direct flame exposure for one hour in a gas-flame application system. The flame-spread diameter upon contact with the underside surface ranged from 15 cm to 20 cm. The temperature was recorded over time every five minutes using an infrared laser device, as shown in Figure 2 (b, c). The ambient temperature and the upper and lower surface temperatures of the sample were recorded at several points on the slabs, as shown in Figure 2 (d), to obtain the curve (temperature-time). The temperature of the flame was also recorded using a thermal valve, as shown in Figure 2 (c), where the flame temperature was $760\text{ }^{\circ}\text{C}$, while the maximum temperature of the concrete surface at the heat source was $600\text{ }^{\circ}\text{C}$ after one hour of the fire. After the completion of the burning process, the samples were removed from the flame-application system and five samples were left to cool in air, while five samples were sprayed with water.

During the combustion phase of a fire, concrete undergoes significant changes. The surface of the concrete exposed to the flames dries out and becomes more porous, which allows the concrete to absorb more

heat. This leads to the formation of thermal cracks, which can widen after the fire is extinguished. If the concrete is cooled too quickly, the thermal cracks can expand further and cause the cementitious layer to delaminate, as shown in Figure 2 (e). A temperature-time curve was obtained by measuring the temperatures of concrete surfaces. This curve can be used to explain the vertical direction of thermal stresses, as the temperatures at points close to heat sources are high, while the temperatures at points far away are low. The slope of the curve is steeper at the beginning of the fire and becomes more linear at the end of the fire and further away from the flame source, as shown in Figure 2 (f).

Rehabilitating Process

Components of Ferro-cement

The ferro-cement mixture was made with the same type of Portland cement and sand, with a sand-to-cement ratio of 2 and a water-to-cement ratio of 0.5. The compressive strength of the ferro-cement was determined by testing 100x100x100 mm cubes after 28 days, which resulted in an average strength of 30 MPa. The metal mesh used was welded and had square openings with dimensions of (25x25) mm and a wire diameter of 2.5 mm, as shown in Figure 3 (a). The tensile-strength test on the metal mesh yielded an average tensile strength of 800 MPa. Steel bolts, 60 mm in length and 5 mm in diameter, shown in Figure 3 (b), were used as shear connectors. The bolts were fastened in the holes drilled on the tile surfaces using a polyester resin material, see Figure 3 (c). A commercially available adhesive material (SBR) was used to bond the ferro-cement to the surface of fire-damaged slabs. The adhesive had a density of $(1.04 \pm 0.01\text{ kg/L})$ at 25°C .

The Method of Implementing the Rehabilitation Process

The damaged slabs were repaired using a ferro-cement layer. A wooden template was placed around each slab to create a 25-mm thick layer. The surface of the tile was roughened using an electric grinder and then coated with a cement slurry containing SBR. The ferro-cement layer was then applied to the surface and leveled with a trowel. For the slabs with eight bolts, four holes were drilled around the main crack and four other holes were drilled around the diagonal cracks. The bolts were then inserted into the holes and secured using a polyester

resin material. The damaged tiles were also reinforced using ferro-cement material with a bonding pattern of twelve bolts or sixteen bolts. Holes were drilled around the cracks in the slabs, at a distance of 5 cm from the cracks. The entire metal mesh, bolts and tile surface

were then sprayed with adhesive material. The ferro-cement mortar was then applied. All slabs were moistened with water for a period of seven days. Finally, the wooden templates were removed, as shown in Figure 3 (d-f).

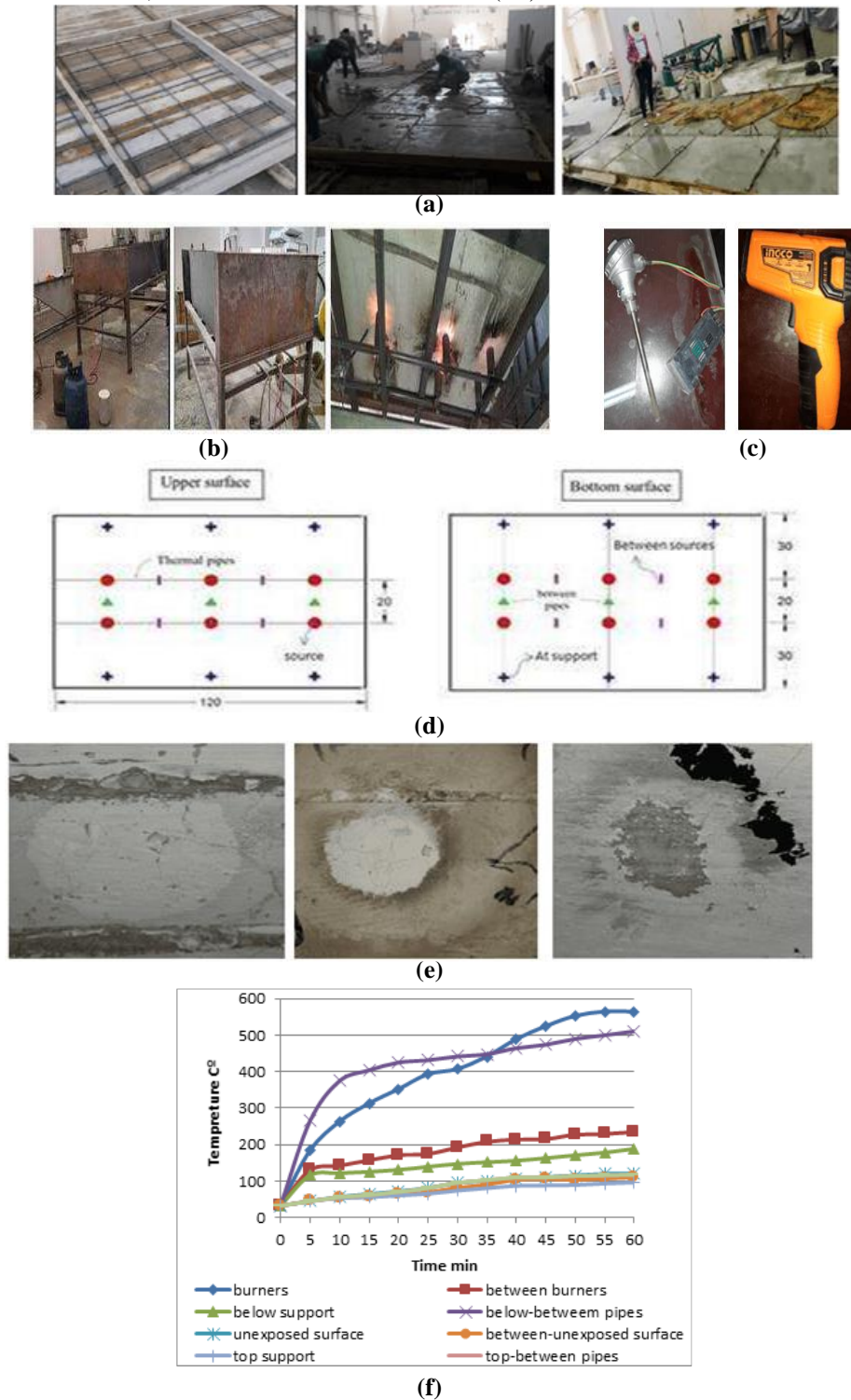


Figure (2): (a) Casting process, (b) Gas furnace, (c) Thermal valve, laser device, (d) Position of the temperature readings, (e) Mechanical response and (f) Temperature-time curve



Figure (3): (a) Metal mesh, (b) Bolts, (c) Polyester maleate, (d) Roughing surface, (e) Location of bolts, (f) Repairing process and (g) Loading device and sensor locations

Model of Loading and Measurement Devices

All specimens were tested using a universal testing machine with a maximum capacity of 200 kN. The test was conducted by applying a concentrated load from the beginning of loading until failure, with a gradual

increase of 5 kN/min at each step. The load at the first crack and the load at failure were recorded for each specimen. The deflections were measured using LVDT sensors placed at the center of the slab, where the maximum deflection is expected to occur. The

transitions in the concrete in the compressed zone were also monitored using the same type of sensors that were fixed on the upper surface of the slab using metal plates at a distance of 12 cm, in order to calculate the value of the deformations, as shown in Figure 3 (g).

RESULTS AND DISCUSSION

Control Slabs

The average collapse load for the two reference slabs was 97.08 kN and the maximum deflection in the center of the slab was 13.35 mm. After determining the average collapse load, the ten other slabs were loaded at 62% of the collapse load, or 60.2 kN, before exposing these slabs to fire, as shown in Figure 4 (b).

Burning Slabs

Load-Deflection Behavior

In this study, the deflections of the reinforced-concrete slabs were monitored under pre-cracking load and ultimate failure load. From Figure 4 (a, b) for all tested slabs, three distinct stages of deflection; namely, pre-cracking, post-cracking and yielding of reinforcements, were observed. The pre-cracking stage starts from zero load to the load of the first crack (linear behavior). The post-cracking stage starts from the load of the first crack to the load of yield of the reinforcement steel (elastic and non-linear behavior). The yielding stage starts from the yield of the reinforcement steel to the failure (plastic and non-linear) (Rosan, 2017). The results obtained reveal that direct flame exposure causes the slabs to lose a portion of their strength and significantly increases the deflection. Figure 4 (b) and Table 2 show that the ultimate bearing capacity of the slabs exposed to direct fire and cooled with air and water decreased by 14.19% and 19.65% respectively, compared to the reference slabs. The deflection at failure increased by 15.56% and 33.08% respectively, for the slabs exposed to fire and cooled with air and water, compared to the reference slabs.

Initial Stiffness and Yielding Stiffness

In this study, two values of stiffness were calculated to represent the behavior of slabs in the elastic and plastic deformation states. The initial stiffness is defined

as the slope of the load-deflection curve from the start of loading to the first-crack load and is calculated from the relationship ($K_{int} = \frac{P_{cr}}{\Delta_{cr}}$), while the post-crack stiffness (yielding stiffness) is defined as the slope of the load-deflection curve from the crack-initiation load to the yield load of the reinforcement steel and is calculated from the relationship ($K_y = \frac{P_y}{\Delta_y}$). Table 2 shows the values of the initial stiffness and post-crack stiffness for the average of the reference specimens and the slabs exposed to fire flame and cooled gradually or suddenly. The initial stiffness of the slabs exposed to fire and cooled gradually and suddenly decreased by 43.7% and 52.8%, respectively, compared to the reference slabs without burning. The stiffness of the specimens at the yield point decreased by 26.8% and 31.7% for the slabs exposed to fire and cooled gradually and suddenly, respectively, compared to the reference slabs. Haddad et al. (2011) studied the behavior of reinforced-concrete slabs by exposing them to heat at a temperature of 600°C for 2h, left one to cool inside the oven and treated the other with water. The researchers found a significant decrease in the resistance of both specimens by 45% compared to the reference and an increase in deflection. The flexural stiffness and durability of the slabs cooled in the oven also decreased by 11% and 53%, respectively, while the flexural stiffness of the water-treated slab increased by 56% and the durability decreased by 32%. The difference between the results of the research and the current study is due to the presence of silica fume in the concrete mixture, which is water-absorbent. Therefore, when cooled with water, the yield strength of the steel can be restored by the absorption of water by the silica fume, meaning that the slab does not lose moisture. In addition, some other mechanical properties are affected when cooled with water.

Ductility Factor

Ductility is the ability of reinforced-concrete (RC) structural members to undergo considerable deformation beyond the yield point without a significant loss of strength. Ductility is measured in this study using two main measures: displacement (DR) and energy absorption.

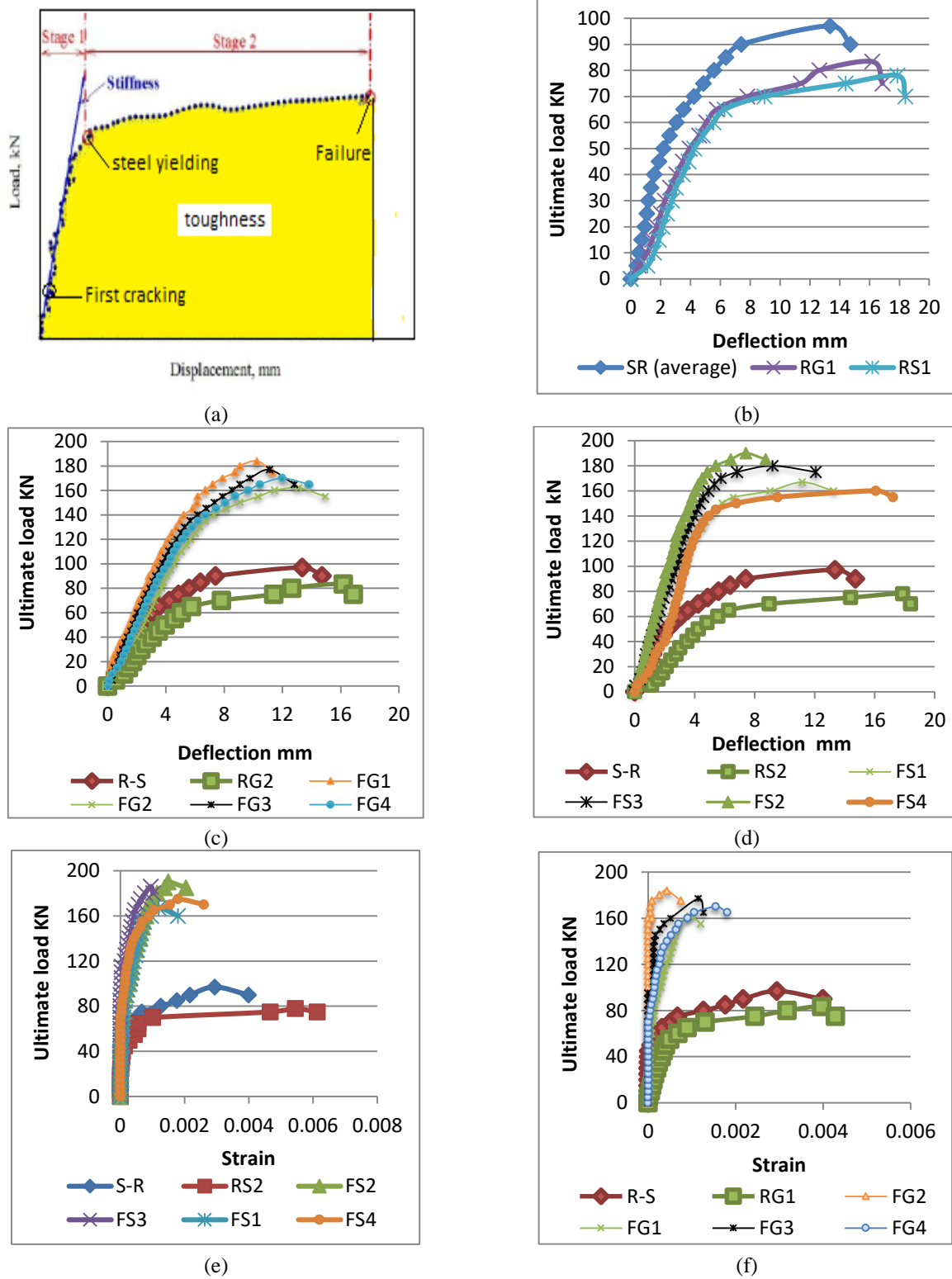


Figure (4): (a) The loading stages of any structural element, (b) Load-deflection curve of burning and cooling slabs compared with the average reference of slabs (unburnt), (c) Load-deflection curve of repairing slabs with ferro-cement for group (2), (d) Load-deflection curve of repairing slabs with ferro-cement for group (3), (e) Load-strain curve of repairing slabs for group (2) and (f) Load-strain curve of repairing slabs for group (3)

Displacement Ductility Factor

The displacement ductility factor is defined as the displacement at the ultimate load divided by the displacement at the yield load $DR = \frac{\Delta_{max}}{\Delta_y}$. According to Table 2, the displacement ductility factor of the slabs exposed to fire flame and cooled gradually and suddenly increased by 6.73% and 11.21%, respectively, compared to the average of the reference samples. The causes of these changes are likely due to the following factors: (a)The thermal expansion of the slabs during the firing process causes the slabs to become more brittle. (b)The cooling process causes the slabs to contract, which can lead to cracking and spalling. (c)The combination of thermal expansion and contraction can cause the slabs to lose their structural integrity.

Energy Absorption Ductility Factor

The energy absorption capacity was calculated as the area under the load-deflection curve. Yielding absorption (post-cracking) and initial absorption (pre-cracking) values were calculated, as shown in Table 2. Exposure of slabs to fire flames leads to a decrease in the amount of absorbed energy. The amount of absorbed energy for the gradually cooled and suddenly cooled slabs decreased by (58%) and (52%), respectively, compared to the average of the reference tiles. This is in agreement with Rosan (2022) who studied the behavior of slabs with openings by exposing them to heat at different temperatures (200°C, 400°C and 600°C). The results indicated that the absorbed energy decreases with increasing temperature according to the following percentages (24, 50.6 and 76.6) %.

Rehabilitating Slabs

Load-Deflection Curves

Figure 4 (c, d) shows the effect of ferro-cement reinforcement on the load-deflection curve. The figure shows that the slope of the curve increases linearly during the first-loading stage (pre-cracking), thus improving the initial stiffness and increasing the first-crack load. When transitioning to the second stage (post-cracking), the slope of the curve increases linearly, but at a slower rate due to the formation of major cracks until reaching the yield point, improving the yield stiffness (post-cracking). Then, we observe a rapid decrease in the slope of the curve until the failure point

for all ferro-cement reinforcement patterns Rosan et al. (2018). This is because ferro-cement reinforcement helps increase the absorbed energy by showing the largest amount of cracks and spreading them slowly with increasing load and reducing deflections. As summarized in Table (3), the results of the loading for these slabs include the load capacity, maximum deflections, ductility factor, initial stiffness and yielding stiffness.

Load Pattern

During the pre-cracking stage, the first-crack load of test slabs was recorded. Table 3 shows that the first-crack load of repaired slabs with ferro-cement according to the bonding patterns (FG1, FG2, FG3 and FG4), respectively increases by (11.11, 40.7, 11.11 and 29.6) % for group (2) and according to the bonding patterns (FS1, FS2, FS3 and FS4) increases by (26.1, 56.5, 43.5 and 43.5) % for group (3) compared to the burnt slabs.

During the post-reinforcement yielding stage, ultimate load of test slabs was recorded. From Table (3), we can conclude an increase in the ultimate load capacity of all repaired damaged slabs using ferro-cement according to different bonding patterns. For group (2): The ultimate load capacity of the slabs repaired with ferro-cement according to the different bonding patterns (FG1, FG2, FG3 and FG4) increases by (94.4, 121, 112 and 104) % and (66.9, 89.5, 82.5 and 75)% compared to the burnt slabs and the unburnt reference slabs, respectively. For group (3): The ultimate load capacity of the slabs repaired with ferro-cement according to the different bonding patterns (FS1, FS2, FS3 and FS4) increases by (114, 144, 138 and 124)% and (72, 95.7, 92 and 82.3)% compared to the burnt slabs and the unburnt reference slabs, respectively.

Deflection Pattern

From Table 3 and Figure 4 (c-d), for the group (2): At ultimate load, the maximum deflections of repaired slabs with bonding patterns (FG1, FG2, FG3 and FG4) decreased by (15, 33.5, 28 and 22.3)%, respectively, compared to the maximum deflections of burnt slabs, while the maximum deflections of repaired slabs with bonding patterns (FG1, FG2, FG3 and FG4) decreased by (3.2, 24.3, 18.1 and 11.5)%, respectively, compared to the maximum deflections of unburnt reference slabs.

Table 2. All results of the average reference slabs and burnt slabs

Slab	P_f	P_u	Δ_u	K_{int}	K_y	Δ_y	D_R	μ_{post}	μ_{pre}	μ_{Ep}	ϵ
	kN		Mm	kN/mm		Mm	-	kN.mm		-	
RS	24	97.1	13.4	21.8	13.7	6	2.2	246	12	20.5	0.003
RG1	27	83.3	16.2	12.3	10	6.8	2.4	231.2	27	8.6	0.004
RS1	23	78	17.9	10.5	9.3	7.2	2.5	241.2	24.5	9.8	0.005

Where: P_f : First-crack load, P_u : Ultimate load, Δ_u : Deflection at ultimate load, K_{int} : Initial stiffness, K_y : Yielding stiffness, Δ_y : Deflection at yielding load, D_R : Ductility factor, μ_{post} : Energy-absorption for the post-cracking stage, μ_{pre} : Energy absorption for the post-cracking stage, μ_{EP} : Energy-absorption factor.

For group (3): At ultimate load, the maximum deflections of repaired slabs with bonding patterns (FS1, FS2, FS3 and FS4) decreased by (37.4, 53, 46 and 38.9)% and (16.2, 25, 13.9 and 2.22)%, respectively, compared to the maximum deflections of burnt slabs and maximum deflections of unburnt reference slabs.

Initial Stiffness, Yielding Stiffness

From Table 3, for group (2): The initial stiffness of the slabs in this group rehabilitated with ferro-cement according to different bonding patterns (FG1, FG2, FG3 and FG4) increased by (61.3, 206, 141.9 and 88.1) % compared to burnt slabs. The initial stiffness of the slabs in group (3) rehabilitated with ferro-cement according to different bonding patterns (FS1, FS2, FS3 and FS4) increased by (84.9, 331, 216 and 162) % compared to burnt slabs. From Table 3, for group (2): The yielding stiffness of the slabs in this group rehabilitated with ferro-cement according to different bonding patterns (FG1, FG2, FG3 and FG4) increased by (91.8, 132, 96 and 100) % compared to burnt slabs. The initial stiffness of the slabs in group (3) rehabilitated with ferro-cement according to different bonding patterns (FS1, FS2, FS3 and FS4) increased by (183.2, 262, 247, 183)% compared to burnt slabs. The results showed that reinforcing damaged slabs with ferro-cement significantly improves the behavior of fire-damaged slabs by improving the stiffness characteristics of all slabs from after the cracking stage until reaching the ultimate load and its ability to slow down the spread of cracks as well.

Ductility Factor

Displacement Ductility Factor

From Table 3, for group (2): The ductility factor of

the repaired concrete slabs according to the bonding patterns (FG1, FG2, FG3 and FG4) decreased by (24.3, 37.4, 31.9 and 37.8) % and by (18.14, 10.5, 27.4 and 18.9) % compared to the ductility factor of the reference slabs and the burnt slabs, respectively. For group (3): The ductility factor of the repaired concrete slabs according to the bonding patterns (FS1, FS2, FS3 and FS4) decreased by (18.15, 10.48, 27.4 and 18.95) % and by (8.9, 1, 19.3 and 9.86) % compared to the ductility factor of the reference slabs and the burnt slabs, respectively.

Energy Absorption Ductility Factor

The absorbed energy of all the rehabilitated slabs with ferro-cement was calculated according to the different bonding patterns as, shown in Table 3. The amount of absorbed energy increases after rehabilitation with vermiculite and with different bonding patterns. The absorbed energy by the ferro-cement-reinforced slabs (FG1, FG2, FG3 and FG4) increased by (172.1, 208, 138 and 168) %, respectively, compared to the burnt slabs (RG1). The absorbed energy also increased by the ferro-cement-strengthened slabs (FS1, FS2, FS3 and FS4) by (132.7, 152, 172 and 71.4) %, respectively compared to the burnt plates (RS1). This explains the ability of vermiculite reinforcement to increase the resistance of the slabs and that the absorbed energy dissipates through a large number of cracks that appear in the reinforced area before reaching failure.

Compression Deformations

From the strain-load diagram in Figure 4 (e, f), we observe a reduction in strains in the compressed-concrete area of the samples reinforced with ferro-

cement according to different bonding patterns. For group (2): The deformations in the concrete of the compressed area of the slabs rehabilitated with ferro-cement according to the bonding patterns (FG1, FG2, FG3 and FG4) decrease by (77, 90, 69 and 59) % and by (69, 80, 59 and 45) % respectively, compared to the burnt slabs cooled by air and water, respectively. For

group (3): The deformations in the concrete of the compressed area of the slabs rehabilitated with ferro-cement according to the bonding patterns (FS1, FS2, FS3 and FS4) decrease by (78, 72, 81 and 67) % and by (59, 48, 66 and 38) %, respectively, compared to the burnt plates cooled by air and water, respectively.

Table 3. All results of repaired slabs

Slab	P_f	p_u	Δ_u	K_{int}	K_y	Δ_y	D_R	μ_{post}	μ_{pre}	μ_{Ep}	ϵ
	kN		Mm	kN/mm		Mm	-	kN.mm		-	
FG1	30	162	13.1	20	19.2	2.99	1.8	525	22.5	23.3	0.0009
FG2	38	184	10.3	38	23.2	1.93	1.49	552	20.9	26.4	0.0004
FG3	30	177	12	30	19.6	2.52	1.62	562.5	15	37.5	0.0012
FG4	35	170	11.1	23.33	20	2.22	1.48	536.5	26.2	20.4	0.0016
FS1	29	167	11.1	19.33	26.36	5.5	2.03	398.7	17.4	22.9	0.0012
FS2	36	190	10.2	45	33.7	4.6	2.22	356.5	14.4	24.8	0.0015
FS3	33	186	9.2	33	32.35	5.1	1.8	398.7	14.8	26.8	0.001
FS4	33	175	11	27.38	26.4	5.5	2.01	420.7	24.7	16.9	0.0018

Crack Patterns

When burnt reference tiles were loaded, they collapsed due to the yielding of the reinforcement steel. The collapse mode was ductile and typical. The slabs first developed a main longitudinal crack in the middle of the tensioned lower surface. As the load increased, additional branching cracks and inclined diagonal cracks appeared. These cracks continued to the upper edges of the slabs and collapse occurred upon reaching the maximum load. The collapse pattern of the burnt reference tiles was similar to that of the reference tiles without burning, as shown in Figure 5 (a). All fire-damaged tiles that were rehabilitated using ferro-cement and following various bonding patterns exhibited the same collapse behavior under the influence of

concentrated external loads. Initially, a network of hairline cracks appeared on the lower surface of the reinforced layer in the bending region. Some of these cracks continued to the supports and then continued vertically to the upper edges of the tiles, leading to the collapse of the reinforced slabs. It was observed that the crack density in the tiles reinforced according to bonding pattern (FG1) was higher than the crack density in the other reinforcement patterns. This suggests that bonding pattern (FG1) is not as effective as the other patterns in preventing the spread of cracks on the reinforced elements. Figure 5 (b) illustrates the crack patterns in some ferro-cement-reinforced concrete samples.

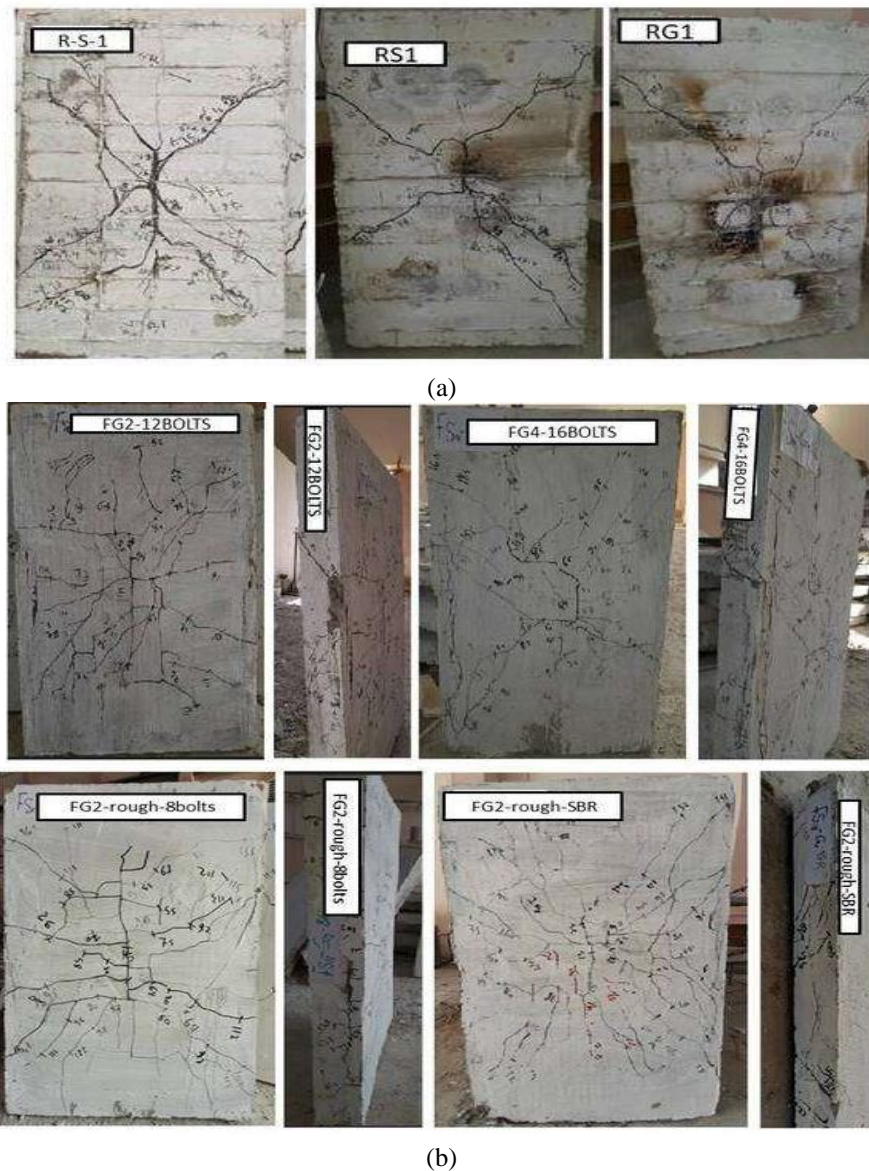


Figure (5): Crack patterns of reference slabs and burnt reference slabs and (b) Crack patterns of repairing slabs with different bounding patterns

CONCLUSIONS

- 1- Exposure to high temperatures and cooling with water and air reduce the load-bearing capacity of slabs and increase deflection.
- 2- The initial stiffness of slabs decreases when exposed to high temperatures. It is also affected by cooling methods, with rapid cooling rates reducing stiffness more than air cooling.
- 3- Exposure to high temperatures reduces the energy-absorption values and cooling methods also affect them. Air cooling reduces energy absorption by (14.9)% compared to water cooling.
- 4- Strengthening of concrete with ferro-cement using different bonding patterns has a significant impact on ultimate load capacity, stiffness, energy-absorption, performance factor, displacement-ductility index and energy-absorption ductility and decreases deflection.
- 5- Regardless of the bonding pattern, strengthening concrete with ferro-cement can reduce crack width and slow down crack propagation.
- 6- Surface roughening is not necessary for ferro-cement reinforcement, as the number of screws or shear connectors can be increased to achieve the same results.

7- The adhesive material (SBR) is effective in ensuring the joint action between the damaged slabs and the reinforcement material.

Acknowledgments

We would like to express our sincere gratitude to all

the authors for their contributions and support throughout this research. We are particularly indebted to the tireless efforts of the first author, Raneen Aldarf, who went above and beyond to ensure the project's success.

REFERENCES

- ACI Committee 549 1R. (2009). "Guide for the design, construction and repair of ferro-cement reported". 93 (Reapproved).
- Ahmad, M. (2013). "Flat-slab reinforcement using ferro-cement to resist shear punching". *Materials Science and Engineering*.
- Ahmed, M.R. (2017). "Repair and strengthening of RC slabs using ferro-cement layers reinforced with different FRP meshes". *Journal of Engineering Research*, 40 (1), 47-57. <https://doi.org/10.21608/erjm.2017.66332>
- Atwan, J.A. (2015). "Evaluation of cement motor-mechanical properties performance: Strengthening by wire mesh (ferro-cement)". *Iraqi Journal of Mechanical and Material Engineering*, 15 (1), 80-94.
- Esmailili, J., Farzam, M., and Baranlou, H.H. (2018). "Investigation on interaction curves of FRP-reinforced-concrete columns". *Jordan Journal of Civil Engineering*, 12 (3), 494-501.
- Fahmy, E., Shaheen, Y.B.I., Abdelnaby, A.M., and Abou Zeid, M.N. (2014). "Applying the ferro-cement concept in the construction of concrete beams incorporating reinforced mortar permanent forms". *International Journal of Concrete Structures and Materials*, 8 (1), 83-97. DOI:10.1007/s40069-013-0062-z.
- Government of Maharashtra. (2018). "Ferro-cement technology". Maharashtra Engineering Research Institute, Nashik 422004, India, 1, 1-152.
- Haddad, R.H., Al-Mekhlafy, N., and Ashteyat, A.M. (2011). "Repair of heat-damaged reinforced concrete slabs using fibrous composite materials". *J. Constr. Build. Mater.*, 25, 1213-1221. <https://doi.org/10.1016/j.conbuildmat.2010.09.033>.
- Handoo, S.K., and Agarwal, S.K. (2002). "Physicochemical, mineralogical and morphological characteristics of concrete exposed to elevated temperatures". *Cement and Concrete Research*, 32 (7), 1009-1018.
- Kanagaraj, B., Anand, N., Andrushia, D., Mathews, M.E., and Alengaram, J. (2022). "Mechanical properties and micro-structure characteristics of self-compacting concrete with different admixtures exposed to elevated temperature". *Jordan Journal of Civil Engineering*, 17 (1). <https://doi.org/10.14525/JJCE.v17i1.01>
- Long, M.J., Man, L.O., and Fan, H.T. (2011). "Experimental research on the strengthening of reinforced-concrete columns by high-performance ferro-cement laminates". *Advanced Materials Research*, 243-249. DOI:10.4028/www.scientific.net/AMR.243-249.1409
- Lugowski, J. (2013). "Ferro-cement super-insulated shell-house design and construction".
- Mabrouk, R., Awad, M., Abdelkader, N., and Kassem, M. (2022). "Strengthening of reinforced-concrete short columns using ferro-cement under axial loading". *Journal of Engineering Research*, 6 (3). DOI:10.21608/erjeng.2022.154329.1083.
- Mathew, G., and Sureshbabu, N. (2021). "Bond-slip behavior of geopolymer concrete after exposure to elevated temperatures". *Jordan Journal of Civil Engineering*, 15 (4), 570-585.
- Mourad, S.E.M. (2006). "Performance of plain-concrete specimens externally confined with welded wire fabric". Research Report, College of Engineering Research Center, King Saud University, Saudi Arabia.
- Obaidat, Y.T. (2018). "The effect of beam design on behaviour of retrofitted beam using CFRP". *Jordan Journal of Civil Engineering*, 12 (1), 149-161.
- Peter, E. (2008). "The analysis of mortars". *Cem. Concr. Inst.*

- Rosan, R. (2017). "Influence of polypropylene fibers on the flexural behavior of reinforced-concrete slabs with different opening shapes and sizes". *Structural Concrete Journal of the FIB*, 19. <https://doi.org/10.1002/suco.201600222>.
- Rosan, R. (2022). "Influence of opening sizes on the flexural behavior of heat-damaged reinforced-concrete slabs strengthened with CFRP ropes". *Case Studies in Construction Materials*, 17, 280-293. <https://doi.org/10.1016/j.cscm.2022.e01464>.
- Rosan, R., Alhassan, M.A., and Alshuqari, E.A. (2018). "Behavior of plain-concrete beams with DSSF strengthened with anchored CFRP sheets: Effects of DSSF content on the bonding length of CFRP sheets". *Case Studies in Construction Materials*, 9 (1). <http://dx.doi.org/10.1016/j.cscm.2018.e00195>.
- Saleem, M., and Ashraf, M. (2008). "Low-cost earthquake-resistant ferro-cement small house". *Pakistan J. Eng. Appl. Sci.*, 2, 59-64.
- Salgia, A.L., and Panganti, A.A. (2018). "Ferro-cement as a cost-effective alternative to RCC". *International Journal of Engineering Research*, 7 (2319-6890), 89-93.
- Sayhood, E., Ali, A., and Sharhan, Z. (2018). "Serviceability limit state of two-way reinforced-concrete slabs strengthened with different techniques". *MATEC Web of Conferences*, 04001, 1-8. <https://doi.org/10.1051/mateconf/201816204001>.
- Shaaban, I.G., Shaheen, Y.B.I., Elsayed, E., Kamal, O.A., and Adesina, P.A. (2018). "Case studies on construction materials' flexural behaviour and theoretical prediction of lightweight ferro-cement composite beams". *Case Studies in Construction Materials*, 9 (June):e00204. DOI:10.1016/j.cscm.2018.e00204
- Shah, S.P. (1974). "Ferro-cement in construction". *Journal of the American Concrete Institute*.
- Sulakhe, P.S., and Awcha, G. (2019). "Effect of fire on concrete and enhancement in fire-resistance capacity of concrete". *International Research Journal of Engineering and Technology (IRJET)*, 6 (5), 2395-0072. DOI: 10.22214/ijraset.2019.6058.
- Waryosh, W.A., and Hashim, H.H. (2020). "Rehabilitation of fire damage-reinforced concrete bubbled slabs". *Journal of Global Scientific Research*, 1, 278-288.